Stem Cell Research & Therapy

RESEARCH

Open Access

Enhancing retention and quality of tissue stromal vascular fraction graft with globo H ceramide

Jing-Yan Cheng[1†], Hui-Yun Cheng[2†], Jung-Tung Hung[1], Gonzalo Mallarino Restrepo[3], Shih-Pin Chiou[1], Ling-Yi Shih[3], Alice L. Yu[1,4,5,6], Huang-Kai Kao[3,4], John Yu[1,4,7*] and Fu-Chan Wei[2,3,4*]

Abstract

Background Fat grafting has been extensively used in plastic surgery practice, yet unstable retention in the recipient site remains a significant clinical challenge. The limited tolerance of injected adipose tissue to ischemia has prompted strategies aiming at timely enhancing the vascularity of the grafted fat. Various modified fat graft preparations have been used, and the mechanically processed tissue stromal vascular fraction (tSVF) derived from fat tissue has garnered considerable interest for enhancing rate of fat graft retention. Further enhancement of the graft retention and quality through supplements to tSVF is worthy of investigation.

Methods The arteriovenous (AV) shunt in rats has been used to evaluate tSVF in vivo. We employed this animal model to investigate the regenerative potential of glycolipid Globo H Ceramide (GHCer) added to tSVF isolated from male Lewis rats. Sixty-two rats divided into four groups were studied. Study parameters included gene expression of vascular endothelial growth factor A (VEGFA) and fatty acid binding protein 4 (FABP4), percentages of the $CD45^{-}CD31^{+}$ endothelial cell, fat tissue retention and fibrotic changes. In vitro studies on adipose-derived mesenchymal stromal cells (AD-MSCs) included angiogenesis by tube formation assay and adipogenesis.

Results The addition of GHCer resulted in superior retention of the tSVF grafts at one-, two-, and eight-week post-grafting ($p < 0.05$). Elevated expression VEGFA was observed from one week ($p < 0.05$), followed by FABP4 at two weeks post-grafting in the tSVF + GHCer grafts ($p < 0.01$). After eight weeks, the numbers of $CD45^{-}CD31^{+}$ endothelial cells and adipocytes were significantly increased in the tSVF + GHCer grafts ($p < 0.01$), while collagen deposition was reduced ($p < 0.05$). Given that GHCer potentially exerted its effects on tSVF through AD-MSCs within, we performed in vitro studies and demonstrated that GHCer promoted AD-MSC differentiation into neovessels ($p < 0.05$) and adipocytes ($p < 0.001$).

†Jing-Yan Cheng and Hui-Yun Cheng contributed equally to this work.

*Correspondence:
John Yu
johnyu@gate.sinica.edu.tw
Fu-Chan Wei
fuchanwei@gmail.com

Full list of author information is available at the end of the article

Conclusions Supplementing GHCer to tSVF effectively reduced fat reabsorption and fibrotic changes of the grafts, while enhancing angiogenesis and adipogenesis, potentially through facilitating AD-MSC differentiation within tSVF. These findings support the potential clinical application of GHCer to enhance the stability and long-term outcomes of fat grafting procedures.

Trial registration Not applicable.

Clinical trial number Not applicable.

Keywords Tissue stromal vascular fraction, tSVF, Globo H ceramide, GHCer, Fat grafting, AD-MSC, AV shunt

Background

Fat grafting is a common practice in plastic and reconstructive surgery to restore soft tissue defects or insufficiency resulting from trauma, cancer ablation or other etiologies. However, whole fat grafting has high resorption rate, primarily due to the inadequate revascularization of the grafted fat within permitted time. Therefore, timely increase of vascularization is conceived as a strategy for successful fat grafting [1].

To improve the retention rate, modified fat grafting techniques have been developed, including methods to process the fat prior to grafting. Tonnard et al. introduced a nanofat technique, which involves disrupting mature adipocytes and emulsifying fat. This approach has shown superior clinical outcomes compared to lipoaspirates that contained intact adipocytes [2]. Characterization of nanofat revealed that it comprises approximately 5% adipocyte-derived stromal cells (AD-MSCs), with adipogenic differentiation potential [2]. Furthermore, since the preparation is solely through mechanical processing, the native extracellular matrix (ECM) and perivascular structures are not fully disrupted, providing physical support for the cells within [3, 4]. This mechanically disrupted fat tissue mixture contains AD-MSCs, endothelial cells, and native ECM while excluding mature adipocytes, is termed tissue stromal vascular fraction (tSVF) [5], a definition supported by the International Federation for Adipose Therapeutics and Science [6].

tSVF can be conveniently prepared and administered to patients in a single surgical procedure. In contrast to culture-expanded AD-MSCs, tSVF involves fewer manipulation, reduces the risk of contamination, and lowers associated costs. The therapeutic potential of tSVF has been demonstrated in wound healing [7], knee osteoarthritis [8], photoaging [9] both in animal models and clinical settings [10].

The in vivo effects of tSVF can be studied via incubation in a closed artificial tissue engineering chamber nurtured by an arteriovenous (AV) shunt. Using a modified nanofat technology in this system [11], Kim et al. observed angiogenesis and adipogenesis of tSVF explants after a six-week period [12]. However, certain percentage of fibrosis was also observed in these explants, which may imply necrosis or reabsorption of the grafted fat tissue [13]. On the other hand, studies have demonstrated that the survival of fat grafts can be improved with the addition of bioactive substances such as prostaglandin E2 and a specific glycoprotein, potentially through enhancing angiogenesis and reduced apoptosis [14, 15]. Enhanced angiogenesis can also protect adipose tissue from hypoxia and fibrosis [16]. Based on these findings, we propose that supplementing tSVF with a pro-angiogenic factor can further improve graft outcome.

Glycosphingolipids (GSLs) encompass a diverse group of membrane glycolipids characterized by a ceramide backbone covalently linked to a glycan moiety. These molecules play crucial roles in various cellular processes during embryogenesis and differentiation [17–19]. We previously demonstrated that globo-series GSLs, such as Globo H ceramide (GHCer), exhibit a restricted expression pattern during early embryonic development and are generally absent in mature cells of normal tissues [20–22]. Furthermore, GHCer can activate human umbilical vein endothelial cells (HUVECs) and facilitate formation of new blood vessels both in vitro and in vivo [23, 24]. These findings suggest potential therapeutic applications of GHCer to enhance angiogenesis in ischemic environments [25].

In this study, we aim to investigate if addition of GHCer can enhance the retention of tSVF grafts and its mechanisms through increased angiogenesis and adipogenesis while simultaneously reducing fibrosis.

Materials and methods

Rats

The male Lewis rats were purchased from the BioLASCO Taiwan CO., Ltd. in Taipei, Taiwan. The rats were housed at the Association for Assessment and Accreditation of Laboratory Animal Care (AAALAC)-accredited animal facility of the Linkou Chang Gung Memorial Hospital, Taiwan, with a 12-hour light cycle and free access to water and rat chaw. The cages were enriched with sterilized non-toxic toys. Experiments were performed on rats with an average weight of 380–420 g and aged 12–14 weeks. Animal studies adhered to the guidelines for the Care and Use of Laboratory Animals and were approved by the Institutional Animal Care and Use Committee of

Linkou Chang Gung Memorial Hospital. This work has been reported in line with the ARRIVE guidelines 2.0.

Collection of fat-derived tSVF

We employed a modified nanofat technology to prepare tSVF from rats [11, 12]. In the Microsurgery Suite of the animal facility at Linkou Chang Gung Memorial Hospital, rats were anesthetized by 5% isoflurane for induction, and were then placed on their backs. Both inguinal areas and legs were clipped and disinfected. One inguinal fat pad was en bloc harvested and immediately processed in the laboratory according to the protocol published by Kim et al. [12]. Briefly, blood vessels and visible connective tissue of the fat pad were cautiously removed, and fat was rinsed with sterile 0.9% saline solution. Next, the fat was finely minced by a scalpel to imitate the fragmentation that fat undergoes during the liposuction procedure in humans. The minced fat was then shifted through a Luer lock connector with an inner diameter of 1.2 mm (Tulip Medical Products) for thirty times. The mechanical force disrupts the mature adipocytes, releasing the fat within the cells and leading to emulsification. The remaining cells, which stayed in the small tissue fragments produced by the mechanical force, were concentrated at the bottom when the emulsified fat was centrifuged at 1200× *g* for 5 min. The resulting pellet at the bottom of the centrifugation tube was the final tSVF. The acquired tSVF volume was generally less than 0.3 ml, and phosphate buffered saline (PBS) was added to bring the total volume to 0.3 ml. The upper layers were discarded.

AV shunt and implantation of tSVF-fibrin hydrogel mix

While the fat was processed, AV shunting was performed in parallel. All surgeries were performed under a surgical microscope in sterile conditions on a heat mat. An AV shunt was created by an end-to-end anastomosis between the distal ends of the deep femoral artery and inferior epigastric vein with 10/0 nylon. The patency was checked. Next, the AV shunt was placed into a PolyJet tissue engineering chamber (total volume of 0.9 mL with a central pin to secure the AV shunt) through a small entrance at one side, and secured by a central pin inside of the chamber. An tSVF-fibrin hydrogel mix containing 0.3 mL of autologous tSVF and 0.3 mL of fibrin hydrogel (10 IU thrombin and 12.5 mg/mL fibrinogen, Sigma-Aldrich) was filled into the chamber containing the AV shunt. The chamber was closed by a lid and secured to the thigh with two 4/0 nylon sutures. Skin closure was completed by interrupted vicryl 4 – 0 sutures. The explants within the chambers were collected after 1, 2, and 8 weeks for further analysis. Following the surgery, the rat was returned to its cage after recovering from anesthesia. The health condition was monitored daily. From the day of surgery, prophylactic medication included 15 mg/kg cefazolin and 2 mg/kg ketoprofen was administered once daily for 3 days, and continued if necessary. If the rat exhibited symptoms of humane endpoints, such as hunched posture, labored breathing, severe vomiting or diarrhea, sudden 20–25% weight loss, and no improvements following treatments, euthanasia was performed using intravenous injection of potassium chloride solution under 4–5% isoflurane anesthesia.

GHCer preparation

GHCer was purchased from TCI Chemicals with a purity greater than 98%. It was dissolved in PBS to a concentration of 2 mg/mL (1.3 mM), aliquoted, and stored at 4 °C until use. For the tSVF and AD-MSC experiments, a final concentration of 20 μM GHCer was used, as this dosage has been previously shown to activate angiogenesis [23, 24].

Study design

A total of sixty-two rats underwent AV shunt surgery (Fig. 1A) and were divided into four groups: Group 1 received tSVF in the chamber (tSVF group), and Group 2 had GHCer mixed with tSVF before placement into the chambers (tSVF + GHCer group). Group 3 received hydrogel only without tSVF in the chamber ($N = 3$), and Group 4 contained hydrogel and GHCer ($N = 3$). Groups 3 and 4 served as the control groups to evaluate the physiological effects of hydrogel and GHCer after in vivo incubation. The first two groups were collected at 1 week, 2 weeks and 8 weeks after surgery, with 8 rats for each time points. In the eight-week groups, four rats were prematurely sacrificed due to thrombosis of the AV shunt, and additional experiments were performed to compensate for the loss ($N = 26$ for Groups 1 and 2 each). Additionally, tSVF from four rats were subjected to RNA isolation immediately after preparation, and served as the naïve RNA control.

Each experimental rat was attached with an ear tag for unique identification. This ear tag system enabled accurate tracking of individual rats throughout the study, minimizing the risk of misidentification and ensuring that treatments and measurements were applied to the correct rats. Additionally, to reduce potential observer bias, both the operators conducting the treatments and those assessing the outcomes were blinded to the group assignments. This was achieved by coding the treatment groups, with the code being revealed only after data analysis.

Adipose-derived mesenchymal stromal cells

Preparation and expansion of AD-MSCs were performed as described previously [26]. Briefly, the inguinal fat pads were collected from male Lewis rats aged between 8 and 10 weeks under anesthesia by isoflurane. The fat tissue

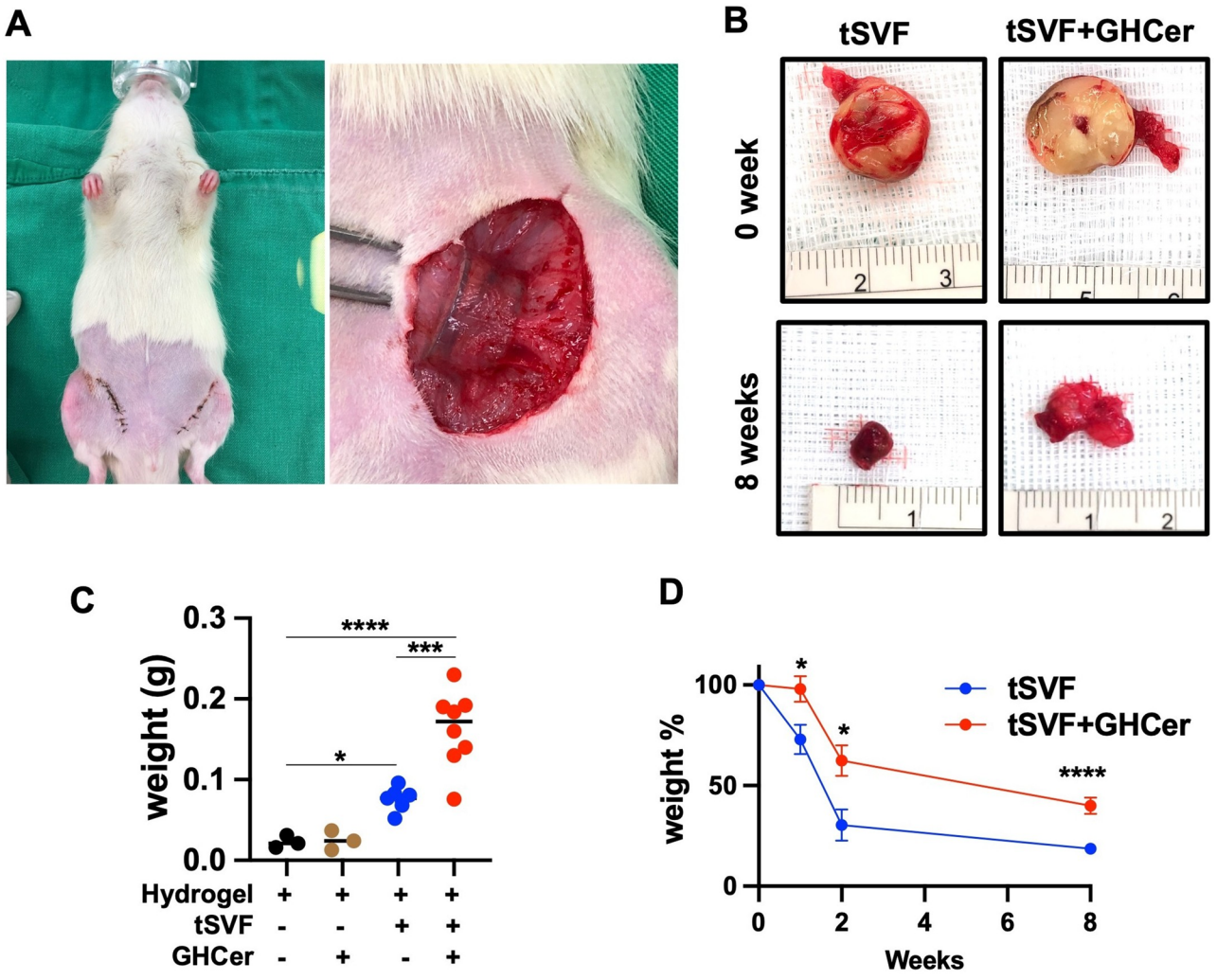

Fig. 1 GHCer enhances the retention of tSVF. (**A**) Fat tissue from right groin was harvested for preparation of tSVF, as described in Materials and methods. On the experimental side (left side), the deep femoral artery and inferior epigastric vein were anastomosed. The AV shunt was then placed into a Poly-Jet tissue engineering chamber, which was filled with a tSVF-fibrin hydrogel mixture and covered by a full lid. Hydrogel was mixed with tSVF, GHCer or tSVF + GHCer respectively, and afterwards engrafted on the left side ($N = 3–8$). The hydrogels were dissected at weeks 1, 2, and 8 following engraftments. (**B**) Photographs of the tSVF/hydrogel mixtures were taken after preparation (0 week) and 8 weeks after engraftment. (**C**) The hydrogels containing specified components were dissected and weighed at 8 weeks after engraftment. (**D**) Percentage change in weight of the tSVF /hydrogel mixture, normalized to the weight measured when freshly prepared at week 0. Except for the tSVF collected at 8 weeks after surgery, which had $N = 7$, all other time points for both the tSVF and tSVF + GHCer groups had $N = 8$. The data are shown as mean ± SD. Statistical significance was assessed using one-way ANOVA with Tukey correction for multiple comparisons or Student's t-test. * $p < 0.05$, *** $p < 0.001$, **** $p < 0.0001$

was then minced and digested with type IV collagenase (Life Technologies) and hyaluronidase (Sigma-Aldrich) for 1 h at 37 °C. The cell pellet was collected and plated in low-glucose Dulbecco's Modified Eagle's medium (DMEM, Life Technologies) supplemented with 10% fetal bovine serum (FBS, Life Technologies) and 1% penicillin-streptomycin (Life Technologies) and incubated at 37 °C in 5% CO_2 atmosphere. The media was replaced every 2–3 days until 80–90% confluence was reached.

Adipogenic differentiation

AD-MSCs were seeded at a density of 1×10^4 cells/cm^2. Cells were incubated in a humidified incubator at 37 °C with 5% CO_2. Adipocyte differentiation was induced by replacing culture medium with adipogenic induction medium (low glucose DMEM supplemented with 1 mM dexamethasone (Sigma-Aldrich), 0.5 mM 3-isobutyl-1-methylxanthine (Sigma-Aldrich), 0.2 mM indomethacin (Sigma-Aldrich), 0.01 mg/ml insulin (Sigma-Aldrich), 10% FBS, and 1% penicillin/streptomycin) in the presence of 20 µM GHCer or PBS, which served as the control since it was the buffer used to dissolve GHCer. The adipogenic induction medium was changed every other day for 14 days.

Oil Red O staining

Frozen sections of grafts or AD-MSC-differentiated adipocytes were fixed in 10% formaldehyde for 30 min at room temperature and washed thrice with distilled water, followed by incubation with Oil Red O working solution (mixed 3 mL of stock solution that contains 5 mg Oil Red O (Sigma-Aldrich) per mL of 60% isopropanol with 2 mL distilled water, and filtered through Whatman filter paper No. 1) for 10 min at room temperature and then washed thrice with distilled water. Cells were examined under the microscope, and images were captured at 10x magnifications using a microscope (DMI 3000, Leica) and analyzed by a StrataQuest software (TissueGnostics). For quantitation of lipid accumulation, cells in each well of the 24-well plate were extracted with 200 µL isopropanol for 10 min, and absorbance at 500 nm was measured using an ELISA plate reader (Thermo Scientific Multiskan Spectrum).

Masson's trichrome staining

Paraffin-embedded tissues were sectioned at 8 µm, rehydrated by a series of incubations in xylene and ethanol solutions and then stained with the Masson's Trichrome staining kit (Sigma-Aldrich) according to the procedures of the manufacturer. The muscle fibers, nuclei, and collagen were stained in red, black, and blue, respectively. Images were acquired using an Aperio digital pathology slide scanner (Leica). Fibrotic area quantification was performed by the StrataQuest software (TissueGnostics). The area of fibrosis was expressed as the percentage of the total specimen areas.

Flow cytometry

To study the cellular composition of the tSVF at the designated endpoint, we minced and digested the tSVF with type IV collagenase (Life Technologies), DNase I (Sigma-Aldrich), and hyaluronidase (Sigma-Aldrich) for 1 h at 37 °C. The resulting cell suspension was centrifuged and the pelleted cells were incubated with anti-CD31 (BD Biosciences) and anti-CD45 (BioLegend) antibodies for 30 min to stain cell-surface antigens. The forward scatter (FSC) versus the side scatter (SSC) plot was applied to gate live cells, excluding cell debris. The CD45 marker was used to detect stromal cells ($CD45^-$), and from these cells to identify the endothelial cells with the phenotype of $CD45^-CD31^+$. Flow cytometric analysis was performed using the SA3800 Spectral Analyzer (SONY), and the data were analyzed with FlowJo software (BD).

Tube formation assay

The growth factor-reduced Matrigel (BD) was placed in 24-well plates and allowed to polymerize for 30 min at 37 °C. Next, AD-MSCs (6×10^4 cells per well) were seeded on the Matrigel and stimulated overnight with the growth factor-enriched EGM2 medium (Lonza) in the presence of GHCer or PBS. After culture for 16 h, images were taken under the microscope (DMI3000, Leica) in 5–8 fields per well. The total length of the tube-like structures, number of branches, nodes (where the branches end or meet) and meshes in the images were quantified by the Angiogenesis Analyzer tool within the Image J software (NIH) [23, 24, 27].

Quantitative real-time RT-PCR

Total RNAs were isolated using Tri-reagent (Invitrogen) according to the manufacturer's instructions. Reverse transcription was performed using the cDNA synthesis Kit (Applied Biosystems). cDNAs were amplified using random primers. Quantitative real-time PCR was performed using SYBR Green Supermix (Applied Biosystems). Primer sequences were listed as follows: VEGFA forward: GAAGACACAGTGGTGGAAGAAG; VEGFA reverse: ACAAGGTCCTCCTGAGCTATAC; FABP4 forward: GTCCT GGTACATGTGCAGAA; FABP4 reverse: CTCTTGTAGAAGTCACGCCT. Samples were run in triplicate in a 96 well Optical Reaction plate (Applied Biosystems). The PCR reaction conditions were 50 °C for 2 min, 95 °C for 5 min, 35 cycles of 95 °C for 30 s, 59 °C for 1 min, 72 °C for 1 min, followed by a dissociation step. Results were analyzed using 7500 fast system Software (Applied Biosystems).

Statistical analysis

Statistical analysis was performed using Prism (GraphPad Software). All values are presented as means ± SD. Three independent experiments were performed for each study, and representative results were shown. Comparison between groups were performed by the Student's t-test or one-way Analysis of Variance (ANOVA) following Shapiro-Wilk's normality test. The asterisk signs designated the probability value reaching statistical significance (*: $p < 0.05$, **: $p < 0.01$, ***: $p < 0.001$, ****: $p < 0.0001$)

Results

GHCer enhanced the retention of tSVF grafts

All the rats had two wounds in the groin area (Fig. 1A left), one was from fat harvest, and the other was from the surgery of AV-shunt and tissue chamber implantation (Fig. 1A right). For the tSVF and tSVF + GHCer groups, the initial wet weight of the tSVF and fibrin hydrogel was approximately 400 mg before being placed to the chamber. Explants were collected at intervals of one, two, and eight weeks after surgery. During the first week postoperatively, it was observed that there were no significant differences in the size of fat grafts between tSVF and tSVF + GHCer groups (Fig. 1B). However, at eight weeks, the graft volume in the tSVF + GHCer group was notably larger than that in the tSVF group (Fig. 1B). As shown, the graft in the tSVF + GHCer group exhibited

soft, fat-like appearance with rich blood supply, while the graft of the tSVF group displayed a hard, grayish, and lackluster texture (Fig. 1B). Furthermore, the grafts in the GHCer group weighed significantly more than those in the tSVF group ($p < 0.001$, Fig. 1C and D). On the other hand, the two control groups, which contained either hydrogel or hydrogel with GHCer, showed minimal remnants after eight weeks, suggesting that neither hydrogel nor GHCer induced physiological effects in our system (Fig. 1C). Moreover, the GHCer group exhibited higher graft weight than the tSVF group at one- and two-weeks post-implantation ($p < 0.05$). This trend persisted when measuring implanted tSVF eight weeks after surgery ($p < 0.0001$) (Fig. 1D). One data point in the tSVF group collected at 8 weeks post-surgery was excluded because it was an outlier, deviating from the third quartile value by more than 1.5 times the interquartile range of the group's data.

GHCer increased the endothelial cells and adipogenesis, but reduced fibrosis

To further investigate the impact of GHCer in tSVF on angiogenesis, single cells were prepared from the grafts after eight weeks in vivo and analyzed with flow cytometry using CD31 as endothelial cell marker and CD45 as hematopoietic cell marker. As shown in one representative experiment in Fig. 2A, the $CD31^+$ cells within the $CD45^-$ population (thus $CD45^-CD31^+$ phenotype) was defined as the endothelial cells. With a total of 8 experiments, we found a substantial increase in endothelial cells from $0.5 \pm 0.7\%$ in the tSVF group to $1.7 \pm 0.8\%$ in the tSVF + GHCer group ($p < 0.01$), strongly supporting the notion that GHCer enhances angiogenesis in grafted tSVF (Fig. 2B).

Secondly, Oil Red O staining was performed to access the lipid content within the grafts (Fig. 3A). The analysis revealed that the tSVF group exhibited an average lipid area of $16.6 \pm 4.7\%$, whereas the tSVF + GHCer group displayed a significantly higher average lipid area of $25.16 \pm 5.1\%$ ($n = 8$, $p < 0.01$) (Fig. 3B). As mature

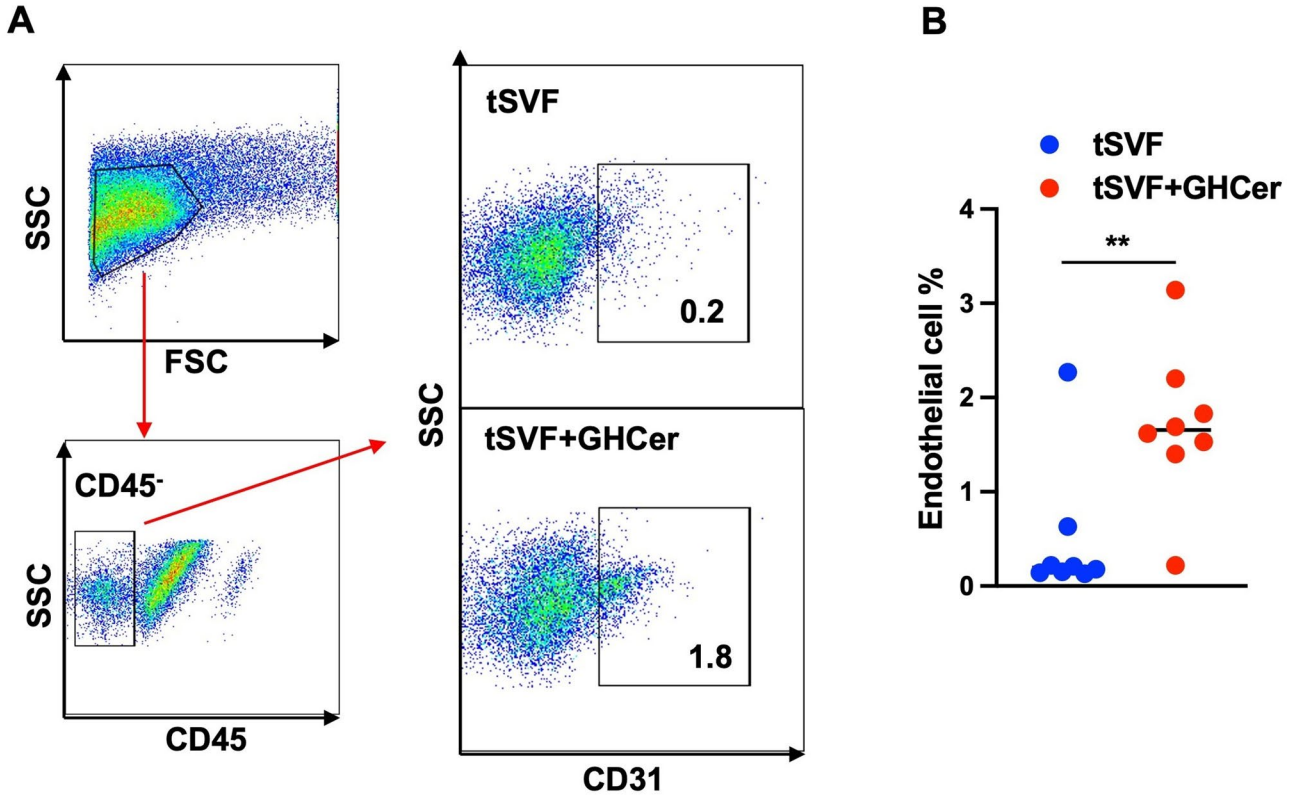

Fig. 2 GHCer increased the percentage of endothelial cells in the engrafted tSVF *in vivo*. tSVF was mixed with hydrogel either alone or in combination with GHCer, and engrafted into the rats for a total of eight weeks before being dissected. (**A**) The dissected mixture was processed to acquire single cell suspension for examination of the $CD45^-CD31^+$ population by flow cytometry. The major live cell population was gated in SSC versus FSC plot for analysis (upper left). Since the percentages of $CD45^-CD31^+$ cells were low, we applied a two-stage gating strategy by first selecting the $CD45^-$ population in the SSC versus CD45 plot (the square in the lower left plot), and then gating the $CD31^+$ population from these $CD45^-$ cells (right panel). The numbers within the squares represent the ratio of $CD45^-CD31^+$ cells in total cell population. (**B**) The percentages of endothelial cells ($CD45^-CD31^+$) among total cells in individual tSVF/hydrogel mixture are presented ($N = 8$). Statistical significance was calculated using Student's t test. ** $p < 0.01$

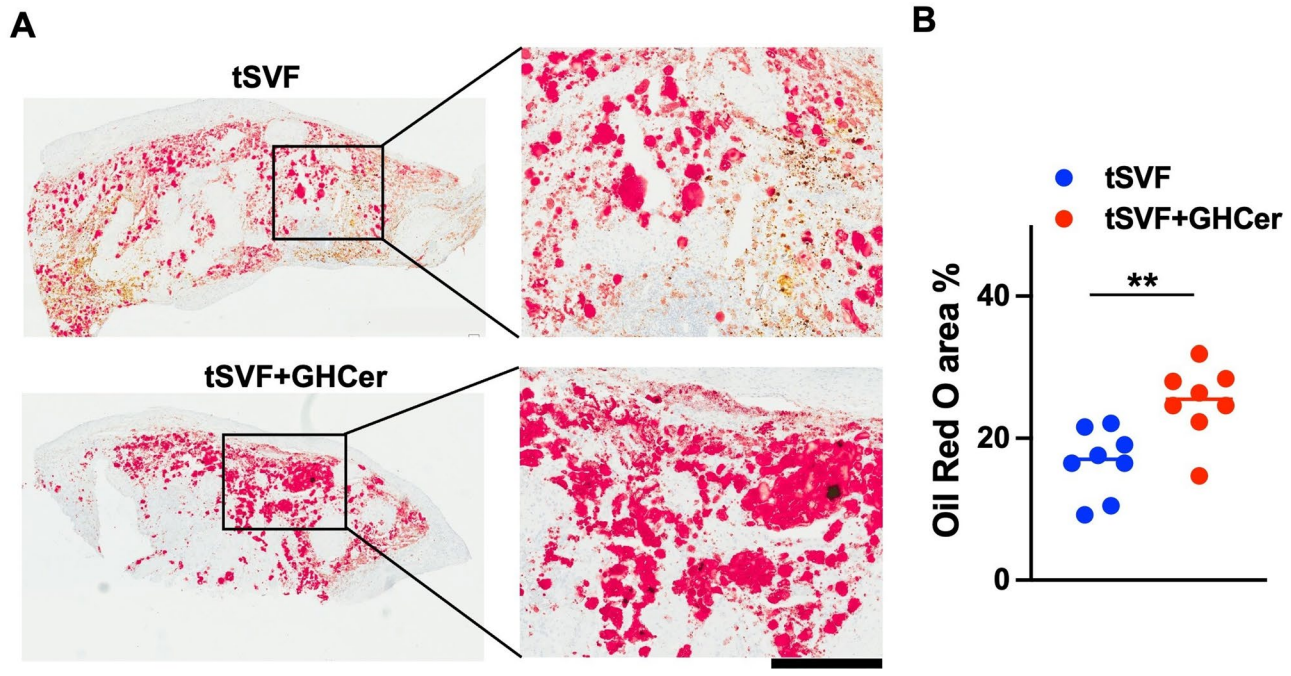

Fig. 3 GHCer increased adipogenesis of engrafted tSVF *in vivo*. tSVF was mixed with hydrogel either alone or in combination with GHCer, and engrafted into the rats for eight weeks before being dissected (**A**) Frozen sections of the dissected grafts were subjected to Oil Red O staining to visualize the lipids (red, scale bar = 200 μm). (**B**) Quantification of lipid areas was conducted and normalized to the total area accordingly ($N = 8$). Statistical significance was acquired using Student's t-test. ** $p < 0.01$

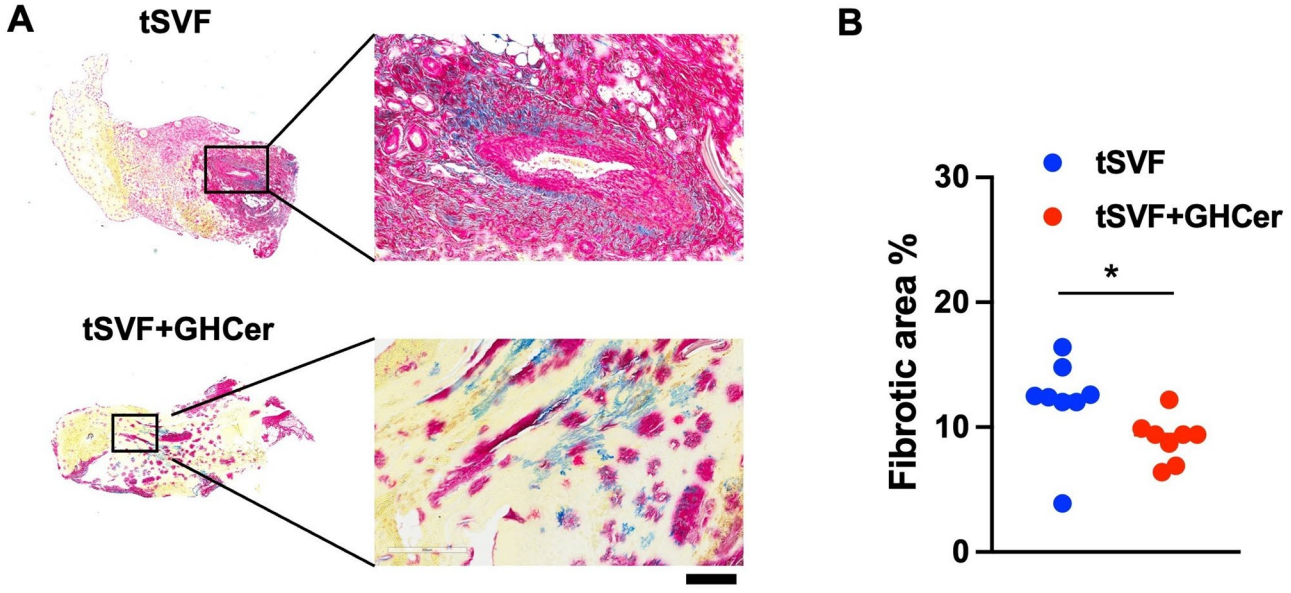

Fig. 4 GHCer reduced fibrosis in the engrafted tSVF *in vivo*. tSVF was mixed with hydrogel either alone or in combination with GHCer, and engrafted into the rats for eight weeks before being dissected ($N = 8$). (**A**) Paraffin sections of the dissected grafts were subjected to Masson's trichrome staining to analyze degree of fibrosis (scale bar = 200 μm). (**B**) Quantification of degree of fibrosis based on the connective tissue and abnormal deposition of extracellular matrix staining (blue) was performed and normalized to the total area accordingly. Statistical significance was acquired using Student's t-test. * $p < 0.05$

adipocytes have been disrupted during preparation of tSVF, our findings support the notion that GHCer enhances adipogenesis in grafted tSVF.

Finally, as angiogenesis and adipose cluster sizes are inversely correlated with extracellular matrix (ECM) deposition [28, 29], we evaluated ECM deposition in the explants. Masson's trichrome staining which analyzed the degree of fibrosis (Fig. 4A) showed that the fibrosis area was 12.1 ± 3.7% and 9.0 ± 1.8% of the total area for the tSVF and the tSVF + GHCer groups, respectively ($n = 8$,

$p < 0.05$) (Fig. 4B). In consequence, the addition of GHCer in the fat graft significantly reduced the degree of fibrosis, a major complication which leads to dysfunction of grafted fat tissue.

Therefore, GHCer promotes angiogenesis and adipogenesis while reducing the degree of fibrosis in grafted tSVF. Our data demonstrate that GHCer enhances the survival and quality of the grafted tSVF.

GHCer promoted angiogenic and adipogenic signals in tSVF in vivo

During fat grafting, neovascularization and adipogenesis are linked intricately through paracrine signaling pathways [30]. To study this relationship, we examined the expression of two pivotal genes crucial for the regeneration of vascular and adipose tissues, the vascular endothelial growth factor A (VEGFA) and fatty acid binding protein 4 (FABP4), during the early stage after tSVF implantation (Fig. 5). Compared to "naive tSVF" which had not been grafted into the animal, tSVF increased 13.8 ± 4.5 fold VEGFA mRNA expression after one week of grafting ($p = 0.75$). Remarkably, the addition of GHCer further enhanced VEGFA expression in tSVF to 23.9 ± 5.7 fold ($p < 0.05$). This trend became even more prominent when analyzing the grafted tSVF after two weeks, with VEGFA expression reaching 19.3 ± 3.6 and 34.3 ± 7.6 folds in the tSVF and tSVF + GHCer groups, respectively (Fig. 5A).

In contrast, the expression of FABP4 in the tSVF treated with/without GHCer remained unchanged in the first week after implantation. However, by the second week, the expression was up-regulated to 5.3 ± 2.0 fold ($p = 0.0892$) in the tSVF group and 12.1 ± 1.9 fold ($p < 0.01$) in the tSVF + GHCer group (Fig. 5B) when compared to "naïve tSVF".

These findings suggest that GHCer enhances angiogenesis and adipogenesis in tSVF by upregulating the expression of the VEGFA and FABP4 genes. Furthermore, the upregulation of VEGFA preceding FABP4 suggests that GHCer initiates an angiogenic signal after tSVF implantation, and the newly formed vessels, in turn, promote adipogenesis.

GHCer enhanced vasculogenic and adipogenic differentiation of AD-MSCs

tSVF encompasses diverse cell types, prominently enriched with AD-MSCs which possess versatile precursor capabilities and demonstrate multilineage differentiation potential [2, 3]. We hypothesized that GHCer mediates angiogenic, adipogenic and anti-fibrotic effects on tSVF through influencing AD-MSCs. To test this hypothesis, we employed the tube formation assay, which is widely used as an in vitro model of angiogenesis, on

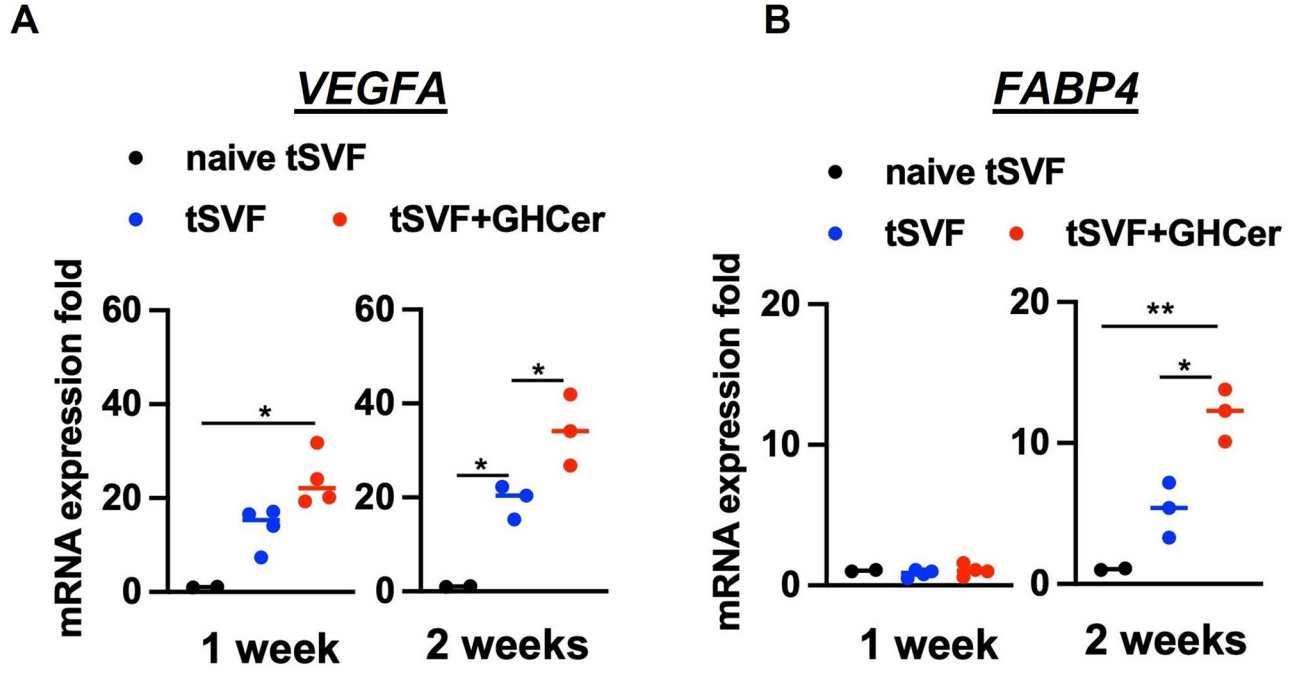

Fig. 5 GHCer increased expression of angiogenic and adipogenic factors in tSVF *in vivo*. tSVF was mixed with hydrogel in the presence or absence of GHCer and engrafted into the rats. Total RNA was extracted from tSVF dissected at the specified time after engraftment to evaluate the gene expression of (**A**) *VEGFA* and (**B**) *FABP4* by real-time quantitative PCR ($N = 4$). The mRNA levels were normalized to those of *GADPH* and shown as fold changes of the freshly prepared tSVF (naïve tSVF) which had not been grafted into the rat. The data are presented as mean ± SD. Statistical significance was calculated using one-way ANOVA with Tukey correction for multiple comparisons. * $p < 0.05$, ** $p < 0.01$

rat AD-MSCs in the presence or absence of GHCer. It was shown that when cultured in the growth factor-rich EGM2 medium, AD-MSCs showed the formation of vessel-like structures (Fig. 6A). Addition of GHCer further augmented the tube formation capacities of AD-MSCs, leading to the elongated tubes and the increased numbers of branches and nodes (Fig. 6B).

We then investigated the potential of GHCer to facilitate the differentiation of AD-MSCs into adipocytes by Oil Red O staining of lipid in cells. In a two-week culture of AD-MSCs in adipogenic differentiation medium, the percentage of Oil Red O positive cells was approximately 5.3 ± 4.3% (Fig. 7A and B). However, the addition of 20 μM GHCer to the medium significantly increased the number of Oil Red O positive cells to 35.3 ± 6.7%. This outcome was further validated by extracting Oil Red O using isopropanol and measuring the absorbance of the solution at 500 nm with a microplate reader. The OD_{500} of the GHCer group (0.40 ± 0.04) was significantly higher than that of the control group (0.13 ± 0.02) (Fig. 7B).

Collectively, our data provides evidence that GHCer significantly improves the retention and quality of grafted tSVF following implantation, with increase of angiogenesis and adipogenesis and decrease of tissue fibrosis. Our data also supports that the supplementation of GHCer to AD-MSC culture promotes vasculogenic and adipogenic differentiation. Taken together, the data highlight the potential of GHCer as one supplement to enhance the tissue regenerative effects of tSVF.

Discussion

The success of fat graft retention at the recipient site requires adequate oxygen and nutrients supply to the adipocytes, which depends on the density of vessels growing into the graft [31, 32]. Conversely, the inhibition of angiogenesis reduces graft retention and impairs adipocyte function [33]. While the strategy of mechanical disruption for tSVF preparation offers advantages, the lower percentage of AD-MSCs in graft may compromise tSVF's proangiogenic potential [34], which may be restored with proper supplements.

Our previous studies on the pro-angiogenic effects of GHCer in human umbilical endothelial cells (HUVECs) [18, 19], together with current findings, affirm its broad angiogenic potential across diverse cell types. Notably, the stable expression of VEGFA in the tSVF + GHCer group during the first two weeks post-implantation suggests that growth factor-associated effects of GHCer can contribute to vascularization of the tSVF graft over time. These findings imply the potential of GHCer as a

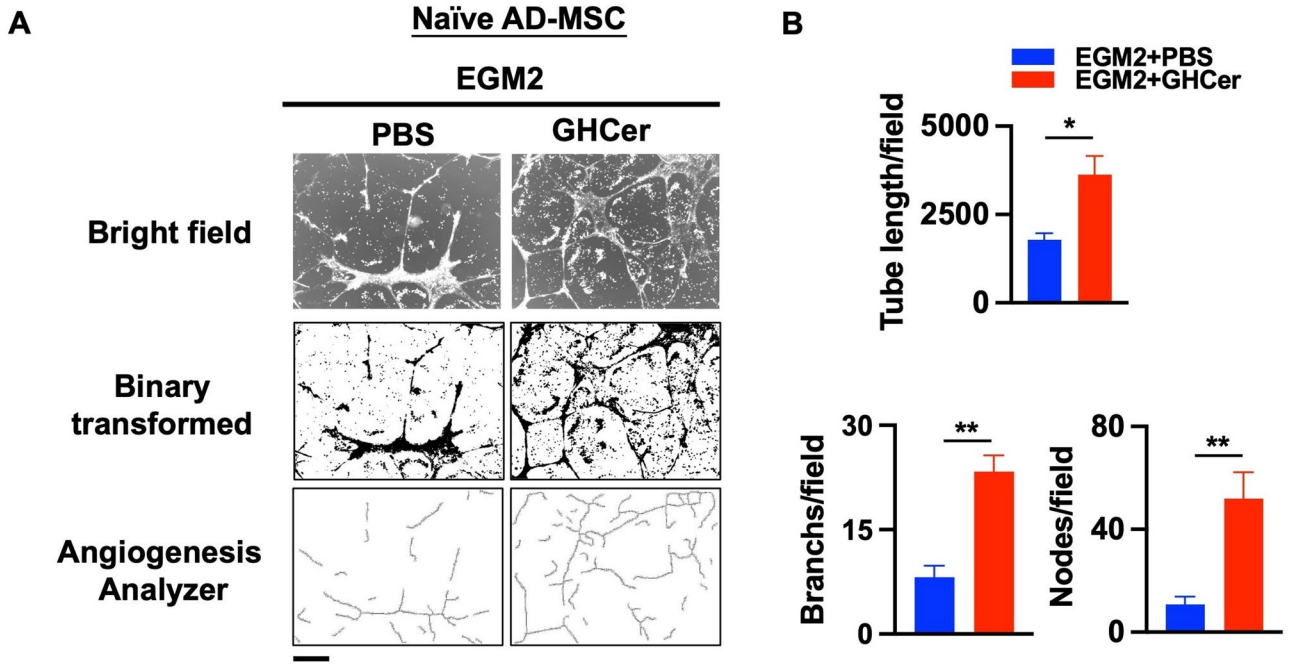

Fig. 6 GHCer enhances angiogenic differentiation of AD-MSCs. (**A**) AD-MSCs were incubated with GHCer or PBS (buffer to dissolve GHCer, served as the control) in growth factor enriched media EGM2 for overnight, and the tube formation was observed using a phase-contrast microscope (scale bar = 100 μm). The bright field photos were transformed to binary images using ImageJ (middle panels) for analyzing the angiogenesis parameters by the Angiogenesis Analyzer plugin in ImageJ. This plugin traced the cells and cell processes from the binary images (bottom panels) and calculated the relevant parameters including numbers of branches (tubes) and nodes (where the branches end or meet), as well as the length of tubes. Each experimental condition was assayed in triplicate and the representative data are shown. (**B**) The total tube length in pixels, number of branches, and number of nodes from the tubes induced by PBS or GHCer were calculated based on four random areas of each well. Values are presented as mean ± SD. Statistical significance was calculated using the Student's t-test. * $p < 0.05$, ** $p < 0.01$

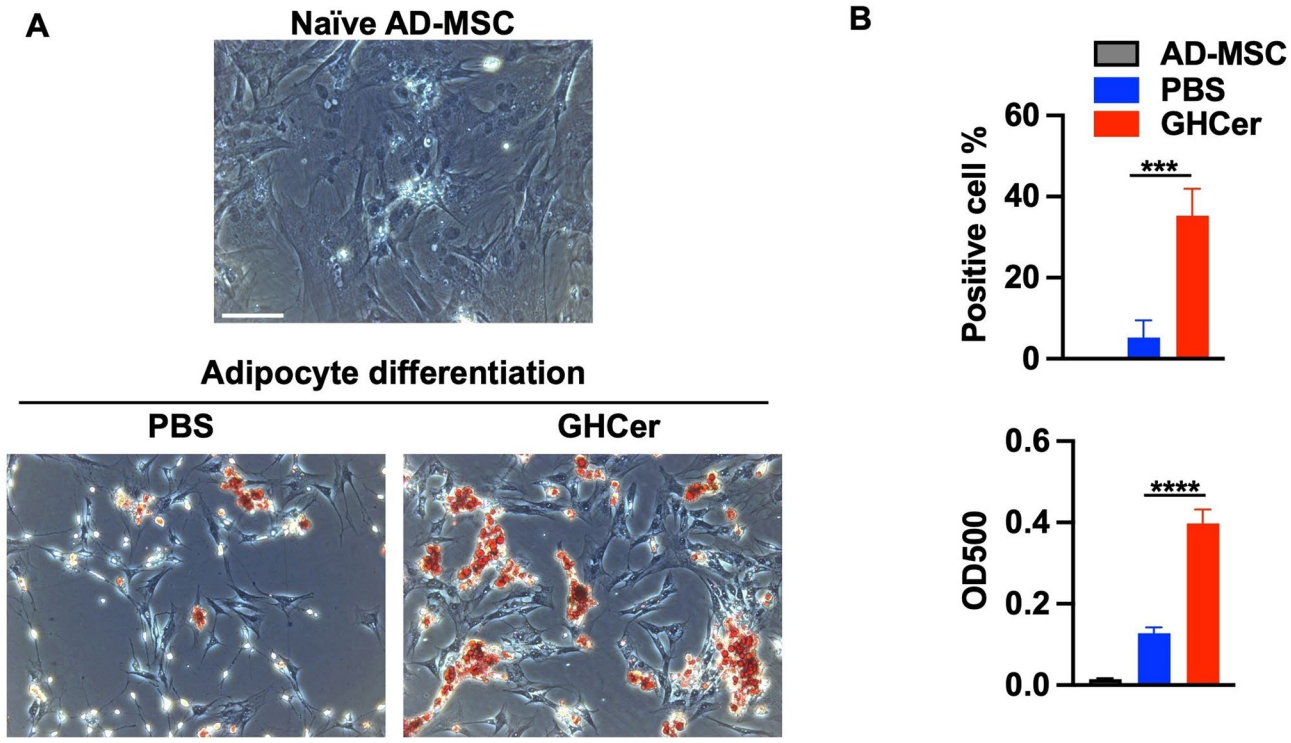

Fig. 7 GHCer enhanced adipogenic differentiation of AD-MSCs. (**A**) AD-MSCs were induced to differentiate into adipocytes for 14 days. The GHCer group was supplemented with 20 μM GHCer in the adipogenic media. These cells were then stained with Oil Red O, and were photographed in 4 fields of each condition under microscope (Scale bar = 100 μm). Each experimental condition was assayed in triplicate and the representative data are shown. (**B**) The percentages of Oil Red O-positive cells in total cell population are presented (upper panel). The accumulated lipids, stained with Oil Red O, were extracted with isopropanol and were quantified with a spectrometer measuring absorbance at the wavelength of 500 nm. Values are reported as mean ± SD. Statistical significance was calculated using the Student's t-test. *** $p < 0.001$, **** $p < 0.0001$

pro-angiogenic agent in clinical applications. By promoting angiogenesis, the grafted tSVF receives more oxygen and nutrients to improve survival and integration into the surrounding environment. Therefore, pro-angiogenic factors like GHCer holds potentials in regenerative medicine and tissue engineering, where augmented angiogenesis is important for successful therapeutic outcomes [35, 36].

Neovascularization and adipogenesis are intricately linked processes [37]. Extensive evidence supports that angiogenesis promotes fat survival and formation [38], while surviving fat promotes revascularization in ischemic tissues [39, 40]. At the cellular level, capillary endothelial cells have been shown to interact with adipocytes and promote adipogenesis [41, 42]. Additionally, the angiogenic growth factors such as VEGFA, have been demonstrated to induce adipogenesis [43–47].

In this study, we demonstrate that GHCer promotes adipogenesis, as evidenced by the upregulation of the adipogenesis marker gene FABP4 two weeks post-implantation and the presence of Oil Red O positive cells resembling adipocytes at eight weeks. Notably, this is the first report showing GHCer's capability to induce adipogenesis. Our previous findings indicated that the angiogenic activity of GHCer is mediated through its interaction with translin-associated protein X [18, 19] and adenosine receptor 2A (A2AR), leading to activation of A2AR and the downstream events (manuscript in preparation). As adenosine has been shown to influence the adipogenic differentiation of bone marrow-derived MSCs [48, 49], it is plausible that the adipogenic activity of GHCer is also mediated by adenosine and A2AR.

Fat grafting outcomes can be compromised by recipient site conditions such as degeneration by aging, trauma, or radiation damage. These factors, along with tissue injuries, edema and hemorrhage that commonly associated with grafting procedure, can trigger proinflammatory responses, leading to chronic inflammation, impaired tissue remodeling and ultimately causing grafted tissue fibrosis [50]. Our data demonstrates that GHCer significantly reduces fibrotic changes of the tSVF graft, making the first report of its anti-fibrosis activity. However, the mechanism through which GHCer modulates fibrosis remains unclear. Since fibrosis often stems from chronic and persistent inflammation, it is reasonable to hypothesize that GHCer helps to create an immunosuppressive microenvironment. As GHCer exhibits significant immunosuppressive activity on T cells [51], potentially

its anti-fibrogenic effects are contingent on these properties. Further experiments are necessary to fully elucidate the exact mechanisms involved.

While the inclusion of GHCer significantly increased tSVF graft retention, we observed a reduction in the total volume of tSVF explants. This decrease could partially result from fibrin hydrogel degradation, as well as insufficient compensation by adipogenesis induced by tSVF and GHCer. Potential modification could involve combining tSVF, GHCer with fat tissues to increase initial graft volume, followed by enhanced angiogenesis and adipogenesis while reducing fibrosis.

It is important to consider the differences in fat composition between humans and rodents when evaluating the clinical applicability of these findings. Many studies have addressed this issue [52], and the rodent inguinal fat pad is considered comparable to human abdominal subcutaneous fat [53]. Additionally, human and rat tSVF share common cellular components, including MSCs, endothelial progenitor cells, and leukocytes, although proportion of each cell type varies with factors such as fat depot, age, sex, and isolation technique [34, 54, 55]. The shared presence of MSCs in both human and rodent tSVF suggest that GHCer may exert similar effects on both. This hypothesis could be further validated with similar experimental setups using human-derived tSVF in immunodeficient rats [56, 57].

Although we have established an animal model to track changes in angiogenesis, adipogenesis and fibrosis of tSVF over a two-month period in vivo, the actual volume changes of the tSVF are limited by the chamber size, which needs to fit in the rat's groin area. Adjustments to the model are necessary to observe real volume changes of the tSVF grafts over an extended period.

Conclusions

Clinical fat grafting faces the challenge of unstable retention due to ischemia resulting from inadequate and timely revascularization within the graft. In this study, we demonstrated that supplementing the tSVF with the glycolipid GHCer significantly enhances both angiogenesis and adipogenesis, while reducing tissue fibrosis. This effect is likely mediated by the function of GHCer to promote the angiogenic and adipogenic differentiation of the AD-MSCs within the tSVF. These findings present a promising strategy to improve the clinical outcome of fat grafting.

Abbreviations

tSVF	Tissue stromal vascular fraction
AV shunt	Arteriovenous shunt
GHCer	Globo H ceramide
VEGFA	Vascular endothelial growth factor A
FABP4	Fatty acid binding protein 4
EPC	Endothelial progenitor cell
GSL	Glycosphingolipid
HUVEC	Human umbilical vein endothelial cell
ANOVA	Analysis of variance
ECM	Extracellular matrix

Acknowledgements

The technical assistance of Dr. Nidal Al Deek in animal model is appreciated. The authors would like to thank Laboratory Animal Center, Linkou Chang Gung Memorial Hospital, for the animal husbandry and care.

Author contributions

J-YC designed and performed experiments, analyzed data, and wrote the original draft of the manuscript. H-YC designed and performed experiments, and wrote and revised the manuscript. J-TH analyzed data and revised manuscript. GMR performed animal experiments. S-PC performed animal experiments. L-YS performed animal experiments. ALY conceptualized the study and substantially revised the manuscript. H-KK established the animal model. JY conceptualized and supervised the study, and revised the manuscript. F-CW conceptualized and supervised the study, and revised the manuscript. All authors read and approved the final manuscript, and confirm their consent for publication.

Funding

This study was supported by grants, MOST 109-2321-B-182A-005 from the Ministry of Science and Technology of Taiwan to JY, and CMRPG1M0031 and CMRPG3N0181-2 from Chang Gung Medical Foundation, Taiwan to F-CW and J-TH., respectively. The funders play no roles in the design, analysis and reporting of the study.

Data availability

The datasets generated and/or analyzed during the current study are available from the corresponding authors on reasonable request.

Declarations

Ethics approval and consent to participate

Animal studies were approved by the Institutional Animal Care and Use Committee of Chang Gung Memorial Hospital at Linkou under two protocols. The first protocol, titled "Effects of the Tumor-derived FACTOR-X on Angiogenesis and Adipogenesis of a Mechanically Isolated Stromal Vascular Fraction (SVF)" was approved with the number 2021080902 on 2021/9/6. The second protocol, titled "Improving the Fat Graft Quality by Globo H Ceramide and Stromal Vascular Fraction" with the approval number 2022021502 on 2022/4/7.

Consent for publication

Not applicable.

Competing interests

The authors declare that they have no competing interests.

Artificial intelligence

The authors declare that artificial intelligence is not used in this study.

Author details

[1]Institute of Stem Cell and Translational Cancer Research, Linkou Chang Gung Memorial Hospital, Taoyuan 333, Taiwan
[2]Center for Vascularized Composite Allotransplantation, Linkou Chang Gung Memorial Hospital, Taoyuan 333, Taiwan
[3]Department of Plastic and Reconstructive Surgery, Linkou Chang Gung Memorial Hospital, Taoyuan 333, Taiwan
[4]Medical College, Chang Gung University, Taoyuan 333, Taiwan
[5]Department of Pediatrics, University of California San Diego, La Jolla, CA92093, USA
[6]Genomics Research Center, Academia Sinica, Taipei 115, Taiwan
[7]Institute of Cellular and Organismic Biology, Academia Sinica, Taipei 115, Taiwan

Received: 17 June 2024 / Accepted: 14 May 2025
Published online: 23 June 2025

References

1. Dong X, Premaratne I, Gadjiko M, Berri N, Spector JA. Improving fat transplantation survival and vascularization with adenovirus E4 + endothelial cell-assisted lipotransfer. Cells Tissues Organs. 2023;212(4):341–51.
2. Tonnard P, Verpaele A, Peeters G, Hamdi M, Cornelissen M, Declercq H. Nanofat grafting: basic research and clinical applications. Plast Reconstr Surg. 2013;132(4):1017–26.
3. Cicione C, Vadalà G, Di Giacomo G, Tilotta V, Ambrosio L, Russo F, et al. Microfragmented and nanofat adipose tissue derivatives: in vitro qualitative and quantitative analysis. Front Bioeng Biotechnol. 2023;11:911600.
4. Alexander RW. Biocellular regenerative medicine: use of adipose-derived stem/stromal cells and it's native bioactive matrix. Phys Med Rehabil Clin N Am. 2016;27(4):871–91.
5. Alexander R. Understanding mechanical emulsification (nanofat) versus enzymatic isolation of tissue stromal vascular fraction (tSVF) cells from adipose tissue: potential uses in biocellular regenerative medicine. J Prolotherapy. 2016;8:e947–60.
6. Trivisonno A, Alexander RW, Baldari S, Cohen SR, Di Rocco G, Gentile P, et al. Intraoperative strategies for minimal manipulation of autologous adipose tissue for cell- and tissue-based therapies: concise review. Stem Cells Transl Med. 2019;8(12):1265–71.
7. Hekimoglu ER, Esrefoglu M, Cimen FBK, Pasin Ö, Dedeakayogullari H. Therapeutic potential of stromal vascular fraction in enhancing wound healing: a preclinical study. Aesthetic Plast Surg. 2025;49(10):2834–49.
8. Vargel İ, Tuncel A, Baysal N, Hartuç-Çevik İ, Korkusuz F. Autologous adipose-derived tissue stromal vascular fraction (AD-tSVF) for knee osteoarthritis. Int J Mol Sci. 2022;23(21):13517.
9. Zheng H, Qiu L, Su Y, Yi C. Conventional nanofat and SVF/ADSC-concentrated nanofat: a comparative study on improving photoaging of nude mice skin. Aesthetic Surg J. 2019;39(11):1241–50.
10. Ghiasloo M, Lobato RC, Díaz JM, Singh K, Verpaele A, Tonnard P. Expanding clinical indications of mechanically isolated stromal vascular fraction: a systematic review. Aesthetic Surg J. 2020;40(9):NP546–60.
11. Pallua N, Grasys J, Kim BS. Enhancement of progenitor cells by two-step centrifugation of emulsified lipoaspirates. Plast Reconstr Surg. 2018;142(1):99–109.
12. Kim BS, Chen SH, Vasella M, Guidi M, Gousopoulos E, Lindenblatt N et al. In vivo evaluation of mechanically processed stromal vascular fraction in a chamber vascularized by an arteriovenous shunt. Pharmaceutics. 2022;14(2):417.
13. Chen X, Deng Z, Feng J, Chang Q, Lu F, Yuan Y. Necroptosis in macrophage foam cells promotes fat graft fibrosis in mice. Front Cell Dev Biol. 2021;9:651360.
14. Hoon SY, Gao J, Xu L, Yu Z, Jiang T, Kang BK, et al. Effect of additive-assisted fat transplantation on fat graft survival rate: a preliminary experimental study based on a rabbit animal model. Ann Chir Plast Esthet. 2021;66(6):440–6.
15. Ho CK, Zheng D, Sun J, Wen D, Wu S, Yu L, et al. LRG-1 promotes fat graft survival through the RAB31-mediated Inhibition of hypoxia-induced apoptosis. J Cell Mol Med. 2022;26(11):3153–68.
16. Michailidou Z, Turban S, Miller E, Zou X, Schrader J, Ratcliffe PJ, et al. Increased angiogenesis protects against adipose hypoxia and fibrosis in metabolic disease-resistant 11β-hydroxysteroid dehydrogenase type 1 (HSD1)-deficient mice. J Biol Chem. 2012;287(6):4188–97.
17. Handa K, Hakomori SI. Changes of glycoconjugate expression profiles during early development. Glycoconj J. 2017;34(6):693–9.
18. Ho MY, Yu AL, Yu J. Glycosphingolipid dynamics in human embryonic stem cell and cancer: their characterization and biomedical implications. Glycoconj J. 2017;34(6):765–77.
19. D'Angelo G, Capasso S, Sticco L, Russo D. Glycosphingolipids: synthesis and functions. FEBS J. 2013;280(24):6338–53.
20. Chang WW, Lee CH, Lee P, Lin J, Hsu CW, Hung JT, et al. Expression of globo H and SSEA3 in breast cancer stem cells and the involvement of fucosyl transferases 1 and 2 in globo H synthesis. Proc Natl Acad Sci USA. 2008;105(33):11667–72.
21. Liang YJ, Kuo HH, Lin CH, Chen YY, Yang BC, Cheng YY, et al. Switching of the core structures of glycosphingolipids from globo- and lacto- to ganglioseries upon human embryonic stem cell differentiation. Proc Natl Acad Sci USA. 2010;107(52):22564–9.
22. Lin RJ, Kuo MW, Yang BC, Tsai HH, Chen K, Huang JR, et al. B3GALT5 knockout alters gycosphingolipid profile and facilitates transition to human naïve pluripotency. Proc Natl Acad Sci USA. 2020;117(44):27435–44.
23. Cheng JY, Wang SH, Lin J, Tsai YC, Yu J, Wu JC, et al. Globo-H ceramide shed from cancer cells triggers translin-associated factor X-dependent angiogenesis. Cancer Res. 2014;74(23):6856–66.
24. Wang SH, Cheng JY, Tsai HH, Lo TC, Hung JT, Lin CC, et al. Conformational alteration in glycan induces phospholipase Cβ1 activation and angiogenesis. J Biomed Sci. 2022;29(1):105.
25. Chen X, Yu W, Zhang J, Fan X, Liu X, Liu Q, et al. Therapeutic angiogenesis and tissue revascularization in ischemic vascular disease. J Biol Eng. 2023;17(1):13.
26. Cheng HY, Ghetu N, Huang WC, Wang YL, Wallace CG, Wen CJ, et al. Syngeneic adipose-derived stem cells with short-term immunosuppression induce vascularized composite allotransplantation tolerance in rats. Cytotherapy. 2014;16(3):369–80.
27. Carpentier G, Berndt S, Ferratge S, Rasband W, Cuendet M, Uzan G, et al. Angiogenesis analyzer for ImageJ - a comparative morphometric analysis of endothelial tube formation assay and fibrin bead assay. Sci Rep. 2020;10(1):11568.
28. Crandall DL, Hausman GJ, Kral JG. A review of the microcirculation of adipose tissue: anatomic, metabolic, and angiogenic perspectives. Microcirculation. 1997;4(2):211–32.
29. Kawaguchi N, Xu X, Tajima R, Kronqvist P, Sundberg C, Loechel F, et al. ADAM 12 protease induces adipogenesis in transgenic mice. Am J Pathol. 2002;160(5):1895–903.
30. Cao Y. Angiogenesis modulates adipogenesis and obesity. J Clin Invest. 2007;117(9):2362–8.
31. Pu LLQ, Discussion. Improvement of the survival of human autologous fat transplantation by using VEGF-transfected adipose-derived stem cells. Plast Reconstr Surg. 2009;124(5):1447–9.
32. Karacaoglu E, Kizilkaya E, Cermik H, Zienowicz R. The role of recipient sites in fat-graft survival: experimental study. Ann Plast Surg. 2005;55(1):63–8. discussion 8.
33. Yamaguchi M, Matsumoto F, Bujo H, Shibasaki M, Takahashi K, Yoshimoto S, et al. Revascularization determines volume retention and gene expression by fat grafts in mice. Exp Biol Med (Maywood). 2005;230(10):742–8.
34. Raposio E, Simonacci F, Perrotta RE. Adipose-derived stem cells: comparison between two methods of isolation for clinical applications. Ann Med Surg (Lond). 2017;20:87–91.
35. Uccelli A, Wolff T, Valente P, Di Maggio N, Pellegrino M, Gürke L, et al. Vascular endothelial growth factor biology for regenerative angiogenesis. Swiss Med Wkly. 2019;149:w20011.
36. Mastrullo V, Cathery W, Velliou E, Madeddu P, Campagnolo P. Angiogenesis tissue engineering: as nature intended? Front Bioeng Biotechnol. 2020;8:188.
37. Dong Z, Peng Z, Chang Q, Zhan W, Zeng Z, Zhang S, et al. The angiogenic and adipogenic modes of adipose tissue after free fat grafting. Plast Reconstr Surg. 2015;135(3):e556–67.
38. Hausman GJ, Dodson MV. Stromal vascular cells and adipogenesis: cells within adipose depots regulate adipogenesis. J Genomics. 2013;1:56–66.
39. Vineberg AM, Shanks J, Pifarre R, Criollos R, Kato Y, Baichwal KS. Myocardial revascularization by omental graft without pedicle: experimental background and report on 25 cases followed 6 to 16 months. J Thorac Cardiovasc Surg. 1965;49:103–29.
40. Castellot JJ Jr., Karnovsky MJ, Spiegelman BM. Differentiation-dependent stimulation of neovascularization and endothelial cell chemotaxis by 3T3 adipocytes. Proc Natl Acad Sci USA. 1982;79(18):5597–601.
41. Varzaneh FE, Shillabeer G, Wong KL, Lau DC. Extracellular matrix components secreted by microvascular endothelial cells stimulate preadipocyte differentiation in vitro. Metabolism. 1994;43(7):906–12.
42. Bouloumié A, Lolmède K, Sengenès C, Galitzky J, Lafontan M. Angiogenesis in adipose tissue. Ann Endocrinol (Paris). 2002;63(2 Pt 1):91–5.
43. Cross MJ, Claesson-Welsh L. FGF and VEGF function in angiogenesis: signalling pathways, biological responses and therapeutic inhibition. Trends Pharmacol Sci. 2001;22(4):201–7.
44. Hu L, Yang G, Hägg D, Sun G, Ahn JM, Jiang N, et al. IGF1 promotes adipogenesis by a lineage bias of endogenous adipose stem/progenitor cells. Stem Cells. 2015;33(8):2483–95.
45. He J, Chen DL, Samocha-Bonet D, Gillinder KR, Barclay JL, Magor GW, et al. Fibroblast growth factor-1 (FGF-1) promotes adipogenesis by downregulation of carboxypeptidase A4 (CPA4) - a negative regulator of adipogenesis implicated in the modulation of local and systemic insulin sensitivity. Growth Factors. 2016;34(5–6):210–6.
46. Wang F, Li H, Lou Y, Xie J, Cao D, Huang X. Insulin–like growth factor I promotes adipogenesis in hemangioma stem cells from infantile hemangiomas. Mol Med Rep. 2019;19(4):2825–30.

47. Lin S, Zhang Q, Shao X, Zhang T, Xue C, Shi S et al. IGF-1 promotes angiogenesis in endothelial cells/adipose-derived stem cells co-culture system with activation of PI3K/Akt signal pathway. Cell Prolif. 2017;50(6):e12390.
48. Ciciarello M, Zini R, Rossi L, Salvestrini V, Ferrari D, Manfredini R, et al. Extracellular purines promote the differentiation of human bone marrow-derived mesenchymal stem cells to the osteogenic and adipogenic lineages. Stem Cells Dev. 2013;22(7):1097–111.
49. Gharibi B, Abraham AA, Ham J, Evans BA. Adenosine receptor subtype expression and activation influence the differentiation of mesenchymal stem cells to osteoblasts and adipocytes. J Bone Miner Res. 2011;26(9):2112–24.
50. Yoshimura K, Aoi N, Suga H, Inoue K, Eto H, Sato K, et al. Ectopic fibrogenesis induced by transplantation of adipose-derived progenitor cell suspension immediately after lipoinjection. Transplantation. 2008;85(12):1868–9.
51. Tsai YC, Huang JR, Cheng JY, Lin JJ, Hung JT, Wu YY, et al. A prevalent cancer associated glycan, globo H ceramide, induces immunosuppression by reducing Notch1 signaling. J Cancer Sci Therapy. 2013;5(7):264–70.
52. Chusyd DE, Wang D, Huffman DM, Nagy TR. Relationships between rodent white adipose fat pads and human white adipose fat depots. Front Nutr. 2016;3:10.
53. Börgeson E, Boucher J, Hagberg CE. Of mice and men: pinpointing species differences in adipose tissue biology. Front Cell Dev Biol. 2022;10:1003118.
54. Hendawy H, Kaneda M, Yoshida T, Metwally E, Hamabe L, Yoshida T, et al. Heterogeneity of adipose stromal vascular fraction cells from the different harvesting sites in rats. Anat Rec (Hoboken). 2022;305(12):3410–21.
55. Frazier T, Lee S, Bowles A, Semon J, Bunnell B, Wu X, et al. Gender and age-related cell compositional differences in C57BL/6 murine adipose tissue stromal vascular fraction. Adipocyte. 2018;7(3):183–9.
56. Akgul Y, Constantine R, Bartels M, Scherer P, Davis K, Kenkel JM. Utility of adipocyte fractions in fat grafting in an athymic rat model. Aesthetic Surg J. 2018;38(12):1363–73.
57. Kamenaga T, Kuroda Y, Nagai K, Tsubosaka M, Takashima Y, Kikuchi K, et al. Cryopreserved human adipose-derived stromal vascular fraction maintains fracture healing potential via angiogenesis and osteogenesis in an immunodeficient rat model. Stem Cell Res Ther. 2021;12(1):110.

Publisher's note